# Calcium Binding Proteins: Optical Stopped-Flow and Proton Nuclear Magnetic Resonance Studies of the Binding of the Lanthanide Series of Metal Ions to Parvalbumin†

David C. Corson, Thomas C. Williams, and Brian D. Sykes*

ABSTRACT: Optical stopped-flow techniques have been used to determine the dissociation rate constants ($k_{off}$) for the lanthanide(III) ions from carp (p*I* 4.25) parvalbumin. For most of the 13 different lanthanides studied, the release kinetics were diphasic, composed of both a fast phase (whose rate varied across the series, $La^{3+} \rightarrow Lu^{3+}$, between the limits $-1.2 \leq \log k_{FAST} \leq -0.7$) and a slower phase (whose rate varied across the series, $La^{3+} \rightarrow Lu^{3+}$, between the limits $-1.2 \geq \log k_{SLOW} \geq -2.9$). In addition, the $La^{3+}$- and $Lu^{3+}$-induced changes in the 270-MHz proton nuclear magnetic resonance spectrum of parvalbumin were used to calculate the dissociation constants for these specific lanthanides from the two high-affinity $Ca^{2+}$ binding sites. The $K_D$ for one site appears to remain constant across the lanthanide series, determined to be $4.8 \times 10^{-11}$ M for both $La^{3+}$ and $Lu^{3+}$. The other site, however, is evidently quite sensitive to the nature of the bound $Ln^{3+}$ ion and shows a strong preference for $La^{3+}$ ($K_{D,La} = 2.0 \times 10^{-11}$ M; $K_{D,Lu} = 3.6 \times 10^{-10}$ M). We conclude from these observations that reports of nearly indistinguishable CD/EF binding site affinities for parvalbumin complexes of the middle-weight lanthanides (i.e., $Eu^{3+}$, $Gd^{3+}$, and $Tb^{3+}$) are quite reasonable in view of the crossover in relative CD/EF site affinities across the lanthanide series.

Of the increasing number of proteins isolated that show the capacity to bind $Ca^{2+}$ ions with relatively strong affinities ($K_D < 10^{-5}$), most contain peptide sequences homologous to the CD and EF calcium binding sites of carp parvalbumin (Kretsinger & Nelson, 1976). Crystals of the p*I* 4.25 isozyme of carp parvalbumin have been analyzed by X-ray diffraction techniques (Kretsinger & Nockolds, 1973), indicating clearly that the two calcium binding domains are each composed of a central aspartic acid/glutamic acid rich loop flanked on either side by a 9–12-residue $\alpha$-helix. The CD site of parvalbumin binds one $Ca^{2+}$ ion in a slightly distorted octahedral geometry: the carboxylate groups of two aspartic acid residues and two glutamic acid residues, the peptide oxygen of one phenylalanyl residue, and the hydroxyl oxygen of one seryl residue provide all six coordinating ligands for this $Ca^{2+}$ ion. The EF site, however, provides only five coordinating ligands for the second $Ca^{2+}$ ion: the carboxylate functions of three aspartic acid residues and one glutamic acid residue plus the peptide oxygen of a lysyl residue. The sixth coordination site of the distorted octahedral complex is accessible to solvent and, presumably, is filled by a water molecule (Kretsinger & Nockolds, 1973).

The affinities with which each of the CD and EF helix–loop–helix sequences binds $Ca^{2+}$ and other metal ions have been extensively studied for a number of parvalbumin isozymes from a variety of species. Although several groups (Potter et al., 1977, 1978; Blum et al., 1977; Haiech et al., 1979; Heizman & Strehler, 1979) have shown that the CD and EF sites of several species bind $Ca^{2+}$ ions with indistinguishingly high affinities ($K_D$ values ranging from $8 \times 10^{-9}$ M to $1 \times 10^{-9}$ M), the affinity of one site of hake (p*I* 4.36) parvalbumin for $Ca^{2+}$ is at least 5 times as great as the affinity of the other site (Haiech et al., 1979).

Studies of the binding of lanthanide(III) ions—which behave much like $Ca^{2+}$ with respect to ligand coordination requirements—to the p*I* 4.25 isozyme of carp parvalbumin similarly point to apparent discrepancies in the reported affinities of the CD and EF sites for various lanthanides. The X-ray crystallographic studies of the isomorphous replacement of $Ca^{2+}$ by $Tb^{3+}$ (Moews & Kretsinger, 1975; Sowadski et al., 1978) showed an increase in electron density only at the EF site at low terbium-to-parvalbumin ratios, which implied the sequential replacement of the two $Ca^{2+}$'s by $Tb^{3+}$ in the crystal. The terbium fluorescence data (Donato & Martin, 1974; Nelson et al., 1977; Miller et al., 1980) studied as a function of $Tb^{3+}$ concentration showed a maximum upon the addition of 1.4–1.8 equiv of $Tb^{3+}$ with quenching at higher $Tb^{3+}$ ratios, and this was taken as evidence for equal displacement of $Ca^{2+}$ from two sites followed by binding of $Tb^{3+}$ to a third weaker site. Cavé et al. (1979) used proton-relaxation enhancement methods to study the binding of $Gd^{3+}$ and reported apparently equal affinities. Rhee et al. (1981) used $Eu^{3+}$ and $Tb^{3+}$ luminescence to study the binding of $Eu^{3+}$ and $Tb^{3+}$ and reported relatively equal displacement of the CD and EF calciums by $Eu^{3+}$ and $Tb^{3+}$. Lee & Sykes (1981), however, studied ytterbium-shifted $^1H$ NMR[1] resonances as a function of $Yb^{3+}$ concentration and found sequential displacement of calcium from the two sites. Corson et al. (1983) used optical stopped-flow kinetic methods and $^{113}Cd^{2+}$ NMR to study the displacement of $Ca^{2+}$ and $Cd^{2+}$ by $Yb^{3+}$ and further supported sequential displacement by this lanthanide.

The studies presented in this paper clearly indicate that the relative affinities in solution of the CD and EF binding sites of carp parvalbumin for metal ions are dependent on the nature of the metal ion used. In particular, for the lanthanide series of ions, those metals higher in the series, such as $Yb^{3+}$, appear

† From the Medical Research Council Group on Protein Structure and Function and the Department of Biochemistry, University of Alberta, Edmonton, Alberta, Canada T6G 2H7. *Received May 6, 1983.* This work was supported by the Medical Research Council Group on Protein Structure and Function and the Alberta Heritage Fund for Medical Research (fellowship to T.C.W.).

[1] Abbreviations: Pipes, 1,4-piperazinediethanesulfonic acid; DSS, sodium 4,4-dimethyl-4-silapentane-1-sulfonate; DTT, dithiothreitol; EDTA, ethylenediaminetetraacetate; SDS, sodium dodecyl sulfate; FID, free-induction decay; NMR, nuclear magnetic resonance; FT, Fourier transform.

0006-2960/83/0422-5882$01.50/0 

to have a markedly greater affinity for the EF site; those near the middle of the series, such as $Gd^{3+}$, show nearly identical affinities for the CD and EF sites. Members at the low end of the series, such as $La^{3+}$, have a higher affinity for the CD site than for the EF site. An explanation for these observations in view of the structural differences and ligand requirements of the CD and EF sites and the dehydration rates for the metal ions is offered.

## Materials and Methods

*Materials.* All chemicals used were high-grade commercial products. The disodium salt of Pipes was obtained from Sigma; KCl (reagent grade) was from American Scientific and Chemical; DTT (electrophoresis purity) and $D_2O$ (99.75 mol %) were from Bio-Rad; DSS was from Merck Sharp & Dohme. Lanthanides were from Alfa Products, Ventron Division, in the form of $LaCl_3 \cdot 6H_2O$. Xylenol orange was from Terochem Labs Ltd. and was found to give consistent and reliable extinction coefficients (Hunt & Ginsburg, 1981), which remained stable over several months.

Carp parvalbumin was isolated by the method of Haiech et al. (1979), which utilizes the heat stability of the protein. The parvalbumin component with a p*I* of 4.25 was easily identified by its ultraviolet absorption spectrum, which has characteristic phenylalanyl absorption maxima at $\lambda$ = 253, 259, 265, and 269 nm and has no absorption maximum in the 280-nm region. Other parvalbumin components and frequently encountered contaminants absorb in this tryptophanyl and tyrosyl region. Isoelectric focusing indicated only one band with a p*I* = 4.25. SDS gel electrophoresis gave only one band in the molecular weight range 10 000–12 000, identical with parvalbumin standards previously isolated (Lee & Sykes, 1981). Parvalbumin so prepared was lyophilized and stored frozen in a desiccator.

*Kinetic and Optical Measurements.* Solutions for kinetic experiments and Job plots were made by weight in buffer solutions of 15 mM Pipes and 0.15 M KCl in double-distilled $H_2O$, adjusted to pH 6.65. Parvalbumin concentrations in these solutions were determined by amino acid analysis and UV absorption spectroscopy with an extinction coefficient of $\epsilon_{259} = 2020\ M^{-1}\ cm^{-1}$. Lanthanide solutions were standardized by titration against EDTA with xylenol orange as an indicator (Birnbaum & Sykes, 1978). Lanthanide–parvalbumin complexes were prepared by the addition of aliquots of the lanthanide solution directly to the solution of the calcium-saturated form of parvalbumin (Martin & Richardson, 1979; Darnall & Birnbaum, 1970) so that the $[Ca^{2+}] \geq$ [parvalbumin] in these experiments. Excess $Ca^{2+}$ has been shown to have no effect on the measured $k_{off}$ for the lanthanides from parvalbumin (Corson et al., 1983).

Stopped-flow kinetic experiments were performed on a Durham Gibson stopped-flow instrument (Model 13002), which was interfaced to a Nicolet Instruments Explorer IIIA digital oscilloscope. All stopped-flow experiments were done in the range of 0.005–0.1 optical density units where the approximation applies that the change in percent transmission is proportional to the change in the optical density. The ambient temperature of the stopped-flow reactions was 23 °C. Reactions with $t_{1/2} \geq 2$ min were also studied on Cary 219 or 118C spectrophotometers. These spectrometers were also used for the Job-plot measurements. All kinetic experiments were followed at 570 nm, with a 10–20-fold excess of xylenol orange (XO) over lanthanide. From previous work, the $\lambda_{max}$ of this dye has been shown to be quite sensitive to the presence of lanthanide ions and changes in pH but relatively insensitive to the presence of calcium ions (Corson et al., 1983).

*Kinetic Analysis.* In the case where two reactions were observed with $k_1 \gg k_2$, conventional kinetic analysis techniques were used to determine both rate constants. However, as these two rate constants became more similar, a computer-executed four-parameter curve-fitting routine was used to determine both $k_1$ and $k_2$ by a nonlinear least-squares fit of the kinetic data to a double-exponential decay function:

$$C = A_1 e^{-k_1 t} + A_2 e^{-k_2 t}$$

where $C$ is the concentration of the lanthanide–XO complex and $A_1$ and $A_2$ represent the contributions to $C$ from the fast and slow reactions, respectively. A similar curve-fitting routine with a single-exponential decay function was used to corroborate the rate constants determined by conventional techniques in cases where $k_1 \gg k_2$. The computer-fitted curves gave more reliable results with less deviation.

*Parvalbumin NMR Samples.* A stock solution (1–2 mM) of the calcium-saturated form of carp parvalbumin (p*I* 4.25) was prepared by dissolving 40 mg of the protein in 2.0 mL of a $D_2O$ solution containing 15 mM Pipes, 0.15 M KCl, and 0.5 mM DSS at pH 7.3. To facilitate the isotopic exchange of all labile hydrogens in the sample, the buffered protein solution was then sealed in a screw-capped polyethylene vial, heated in a hot water bath to 60 °C for 10 h, and lyophilized. After a second 2.0-mL portion of $D_2O$ was added, the heat treatment was repeated and the sample again lyophilized. To this twice-exchanged sample, a third and final 2.0-mL aliquot of $D_2O$, and sufficient DTT to give a concentration of 5 mM, was added. Finally, the protein solution was centrifuged. The pH of this sample was determined to be 6.8 with an Ingold glass electrode servicing a Radiometer/Copenhagen PHM62 pH meter. Accurately measured aliquots were hydrolyzed and submitted for amino acid analyses. The protein concentration of the parvalbumin solution was then calculated from the integrated peak areas of the alanine and leucine residues.

*Lanthanide NMR Solutions.* Stock lanthanum and lutetium solutions (approximately 50 mM) were prepared by dissolving approximately 40 mg of their hydrated chloride salts in 2.0 mL of $D_2O$ containing 15 mM Pipes and 0.15 M KCl (previously adjusted to pH 7.3 for the $Lu^{3+}$ solution and to pH 6.8 for the $La^{3+}$ solution). These solutions were twice lyophilized from $D_2O$. The final pH of both solutions was determined to be between 6.6 and 6.8. Their concentrations were determined by titration against EDTA with xylenol orange as an indicator (Birnbaum & Sykes, 1978).

*Acquisition of NMR Spectra.* For each titration experiment, a carefully measured aliquot (approximately 400 $\mu$L using a calibrated 1.0-mL glass syringe fitted in a microtitrator apparatus) was dispensed directly into a 5-mm NMR tube. After an initial spectrum of the protein was acquired, successive additions (approximately 2.5 $\mu$L each) of the particular lanthanide solution were then dispensed directly into the protein solution via a calibrated 100-$\mu$L glass syringe fitted to the microtitrator.

$^1$H NMR spectra were acquired on a Bruker HXS-270 spectrometer operating in the conventional pulsed FT mode with quadrature detection under Nicolet software control. To improve the resolution, samples were maintained at 55 °C. The transmitter pulse was centered between the dominant buffer resonance and the residual HDO line so that fold-over artifacts arising from these two regions did not distort the remainder of the observable spectrum. A Bessel filter set at twice the sweep width (i.e., ±4000 Hz) was employed. For each spectrum, a simple one-pulse sequence [an 8-$\mu$s (70°) pulse followed by an (acquisition plus delay) interval of 2.5 s] was used to collect 2000 FID's in a block-averaged format

after a 30-min temperature equilibration period. Postacquisition processing included resolution enhancement by apodization of the FID's with a double-exponential function. All chemical shifts are referenced to the principal resonance of DSS. The base line for each spectrum was flattened with an interpolating polynomial function, and the resultant spectrum was checked by comparing the integrated areas of the upfield aliphatic (2.5 to −0.5 ppm) and aromatic (8.0–5.0 ppm) regions to the values calculated from the amino acid composition of parvalbumin (assigning the methyl doublet at approximately −0.37 ppm an area of 3).

*NMR Data Analyses.* The dissociation constants of the two lanthanide ions relative to calcium for both the CD and EF metal binding sites of parvalbumin were determined by plotting the normalized peak heights of selected upfield (0.7 to −0.5 ppm) methyl resonances vs. the $[Ln]_0/[parvalbumin]_0$ ratio. A curve-fitting program based on the calculation of the relative concentrations of parvalbumin–metal species present during the titration experiments was then employed to search for the best fit values of the dissociation constants by a least-squares routine.

## Results

*Kinetic Measurements.* Stopped-flow optical kinetic measurements were used to measure the off-rate constants for lanthanides bound to the CD and EF metal binding sites of parvalbumin. The methodology involves mixing the lanthanide parvalbumin complex with a great excess of xylenol orange, a dye that both chelates lanthanides and undergoes an optical spectral change when the lanthanides are bound. Previous measurements of complexes of $Yb^{3+}$ and parvalbumin (Corson et al., 1983) showed that the $Yb^{3+}$'s released from parvalbumin were kinetically distinguishable, one $Yb^{3+}$ being released faster ($k_{off} = 0.15\ s^{-1}$) than the other $Yb^{3+}$ ($k_{off} = 1.3 \times 10^{-3}\ s^{-1}$) at 23 °C and pH 6.6. These measurements were also correlated with $^1H$ NMR measurements on the same system (Corson et al., 1983; Lee & Sykes, 1981). In this paper, we extend these measurements to 13 members of the lanthanide series and correlate the results with the measurements of the off-rate constant for calcium by Potter et al. (1978).

Before proceeding to the kinetic measurements of the parvalbumin system, it is important to characterize the interaction of the other lanthanides with the chelator/indicator xylenol orange. We used Job's method of continuous variations to investigate the stoichiometry of the binding of the lanthanides to xylenol orange (Corson et al., 1983). Job plots were constructed for the entire lanthanide series except $Ce^{3+}$ and $Pm^{3+}$. The total concentrations of lanthanide and xylenol orange used in these experiments was $3.08 \times 10^{-5}$ M, at pH 6.6 and 23 °C. Typical plots have been presented elsewhere (Corson et al., 1983). The first four lanthanides of the series that we examined ($La^{3+}$, $Pr^{3+}$, $Nd^{3+}$, and $Sm^{3+}$) have plots indicating a one-to-one stoichiometry of the lanthanide–xylenol orange complex. This is in agreement with the results published by Tonosaki & Otamo (1962), who found one-to-one binding for $La^{3+}$, $Ce^{3+}$, and $Nd^{3+}$. The results for the rest of the lanthanide series ($Eu^{3+} \rightarrow Lu^{3+}$) indicated a one-to-two lanthanide–xylenol orange complex. The overall indicator dissociation constant calculated from the Job plot for the case of $Yb^{3+}$ was approximately $10^{-11}$ $M^2$.

The off-rate constants for various lanthanides bound to the CD and EF binding sites of parvalbumin were measured by mixing the lanthanide parvalbumin solution with a xylenol orange solution and following the appearance of the xylenol orange lanthanide complex (Corson et al., 1983). When the xylenol orange is in great excess ([XO] ≥ 10–20 × the total

Table I: Measured Off-Rate Constants for Dissociation of Lanthanides from Carp Parvalbumin at pH 6.6 and 23 °C in 15 mM Pipes–0.15 M KCl

| lanthanide | $k_{off}^{EF}$ ($\times 10^{-3}$ $s^{-1}$) | $k_{off}^{CD}$ ($\times 10^{-3}$ $s^{-1}$) | lanthanide | $k_{off}^{EF}$ ($\times 10^{-3}$ $s^{-1}$) | $k_{off}^{CD}$ ($\times 10^{-3}$ $s^{-1}$) |
|---|---|---|---|---|---|
| $La^{3+}$ | 61 | | $Tb^{3+}$ | 7.0 | 97 |
| $Ce^{3+}$ | | | $Dy^{3+}$ | 5.4 | 119 |
| $Pr^{3+}$ | 32 | | $Ho^{3+}$ | 5.0 | 124 |
| $Nd^{3+}$ | 26 | | $Er^{3+}$ | 2.5 | 175 |
| $Pm^{3+}$ | | | $Tm^{3+}$ | 2.0 | 148 |
| $Sm^{3+}$ | 15.7 | | $Yb^{3+}$ | 1.3 | 146 |
| $Eu^{3+}$ | 16.4 | 94 | $Lu^{3+}$ | 1.2 | 179 |
| $Gd^{3+}$ | 13.0 | 90 | | | |

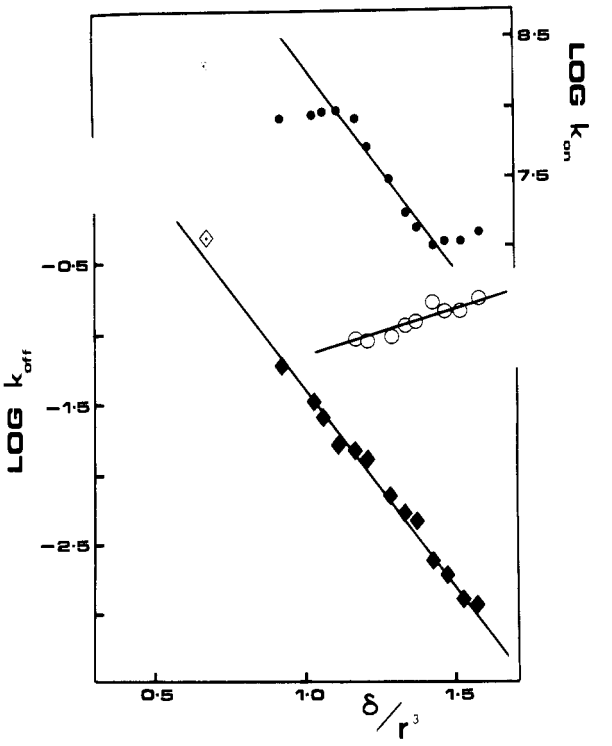


FIGURE 1: Values of logarithm of off-rate constant for dissocation of various lanthanides from the CD (○) and EF (♦) sites of parvalbumin, measured at pH 6.6 and 23 °C in 15 mM Pipes–0.15 M KCl, are plotted vs. ratio of the formal charge on the metal ion to the cube of its ionic radius (Shannon, 1976). Also plotted is the off-rate constant measured by Potter et al. (1978) for the dissociation of calcium from parvalbumin (dotted open diamond) and the dehydration rate constants for calcium (⊙) and for the members of the lanthanide series (●) (Geier, 1965; Diebler et al., 1969). The off-rate constants are plotted relative to the left-hand axis; the dehydration rate constants are plotted relative to the right-hand axis.

$[Ln^{3+}]$), as many as three distinct reactions can be seen depending upon the lanthanide-to-parvalbumin stoichiometry and the particular lanthanide studied. For $Yb^{3+}$ (Corson et al., 1983) and the other heavy lanthanides ($Eu^{3+} \rightarrow Lu^{3+}$), two different first-order reactions could be measured when the lanthanide-to-parvalbumin ratio was 2 or less. The rate constants for these two reactions are listed in Table I and plotted vs. the charge density of the metal ion (see Discussion) in Figure 1. The details of the computer data analysis used to obtain the rate constants are discussed under Materials and Methods. In experiments where the lanthanide-to-parvalbumin ratio exceeded 2, a third reaction, whose intensity increased with increasing lanthanide concentration, was observed. This reaction displayed pseudo-first-order kinetics and, when measured under similar conditions ([XO] ≃ $2 \times 10^{-5}$ M, pH 6.6 and 23 °C), had the same pseudo-first-order rate constant (13 $s^{-1}$) as the reaction XO + La·XO ⇌ $La(XO)_2$. For the

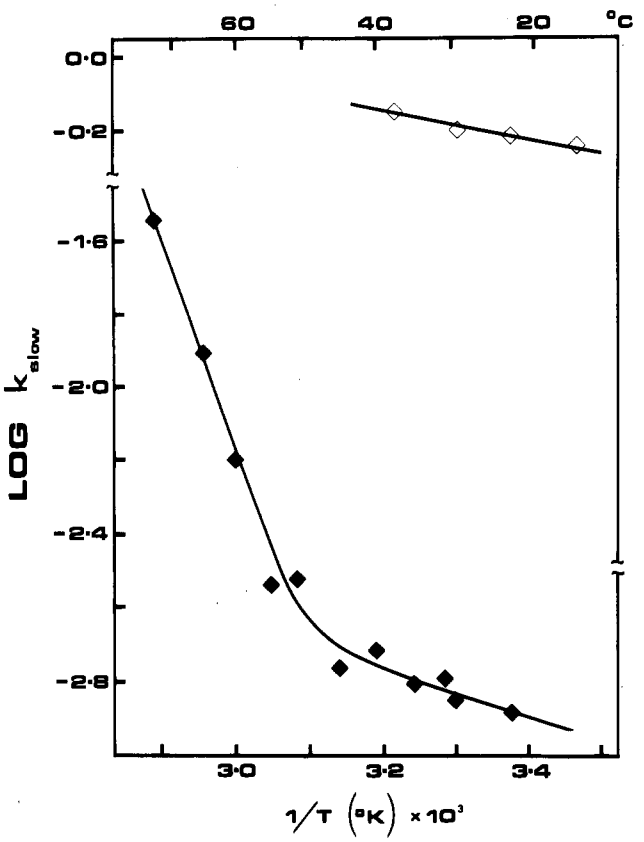


FIGURE 2: Arrhenius plots for off-rate constants for dissociation of $La^{3+}$ (◊) and $Yb^{3+}$ (♦) from the EF site of parvalbumin, measured at pH 6.6 in 15 mM Pipes–0.15 M KCl.

lanthanides at the lighter end of the series ($La^{3+} \rightarrow Sm^{3+}$), when the lanthanide-to-parvalbumin ratio was 2 or less, the difference between the fast and slow off-rate constants precluded the accurate measurement of the fast rate constant, allowing only the slow rate constant to be measured (Table I and Figure 1).

The slow off-rate constants for $La^{3+}$ and $Yb^{3+}$ from parvalbumin were also measured as a function of temperature. Arrhenius plots of the results are shown in Figure 2. The plot for $Yb^{3+}$, performed over a temperature range of 23–70 °C, is clearly nonlinear. The activation energy determined for $Yb^{3+}$ in the low-temperature range (23–50 °C) is 2.6 kcal $mol^{-1}$. The experimentally measured $k_{off}$ at 55 °C is $2.9 \times 10^{-3}$ $s^{-1}$, only 2.2 times larger than the measured $k_{off}$ at 23 °C. The activation energy for $La^{3+}$ measured over the temperature range 15–38 °C is only 1.6 kcal $mol^{-1}$.

*NMR Studies.* The diamagnetic $La^{3+}$ and $Lu^{3+}$ ions compete with and replace the $Ca^{2+}$ ions bound to the metal binding sites of native parvalbumin. Lanthanide titrations of $Ca^{2+}$-saturated parvalbumin thus generate a mixture of parvalbumin–metal complexes. If one assumes that the binding affinity of one site is not influenced by which metal is in the other site, the equilibria interconverting these species (see Figure 3) are simply described by the two relative dissociation constants $K^{CD}$ and $K^{EF}$, defined as follows:

$$K^{CD} \equiv K_{D,Ln}{}^{CD}/K_{D,Ca}{}^{CD} \qquad K^{EF} \equiv K_{D,Ln}{}^{EF}/K_{D,Ca}{}^{EF}$$

where $K_{D,Ln}{}^{CD}$ and $K_{D,Ln}{}^{EF}$ are the dissociation constants for $Ln^{3+}$ from the CD and EF sites, respectively, and $K_{D,Ca}{}^{CD}$ and $K_{D,Ca}{}^{EF}$ are the dissociation constants for $Ca^{2+}$ from the CD and EF sites, respectively (Lee & Sykes, 1981; Sowadski et al., 1978).

The great utility of $^1H$ NMR methods as applied to this problem is the potential for differentiating between the various

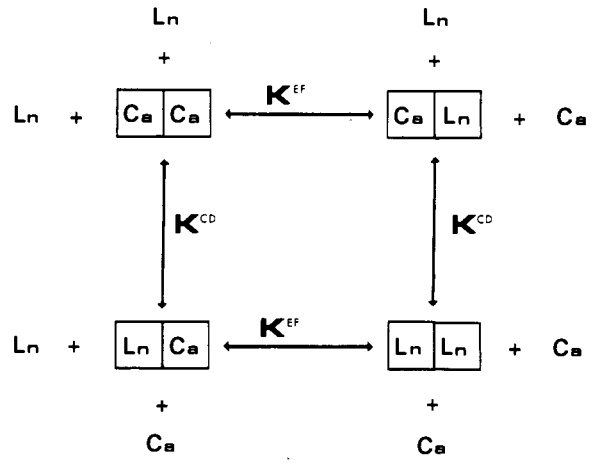


FIGURE 3: Equilibrium interconversions of the four metal-bound parvalbumin species generated by titration of the calcium form with lanthanide(III) ions. The double square represents parvalbumin: the left-hand square indicates the CD site, and the right-hand square indicates the EF site. The four equilibria are interconnected by one-step dissociations: the dissociation constant superscript refers to the protein site undergoing exchange. Apo- and semiapoparvalbumin species are assumed to be present only at negligible concentrations.

parvalbumin–metal complexes involved. In principle, parvalbumin possesses four classes of amino acid residues: those residues sensitive only to the exchange of metal ion at the CD site, those residues sensitive only to the exchange of metal ion at the EF site, those residues sensitive to metal ion exchange at both the CD and EF sites, and those residues insensitive to metal ion binding at either site. The $^1H$ NMR resonance intensity of a residue sensitive only to metal exchange at the CD site reflects that proportion of parvalbumin that remains unexchanged at either site plus that exchanged only at the EF site. Likewise, the resonance intensity of a residue sensitive only to EF site exchange represents that proportion of parvalbumin that remains unexchanged at either site plus that exchanged only at the CD site. Lastly, the resonance intensity of a residue sensitive to exchange at both sites represents only that portion of parvalbumin that has not undergone exchange at either site. Thus, for example, the relative intensities of the unshifted and shifted resonances corresponding to a residue sensitive only to EF site exchange reflect the sum of the concentrations of the CC and LC species and of the CL and LL species, respectively [adopting the shorthand notation of Lee & Sykes (1981) and Sowadski et al. (1978) where CL indicates calcium bound at the CD site and a lanthanide bound at the EF site; see Figure 3].

The upfield-shifted methyl region of native parvalbumin (from approximately –0.4 to 0.6 ppm) exhibits several well-resolved doublet resonances (Figures 4 and 5). These resonances provide an excellent means by which the titration of parvalbumin with $La^{3+}$ or $Lu^{3+}$ can be monitored. Unlike their paramagnetic counterparts, these diamagnetic lanthanide ions do not induce large shifts of the protein resonances (at most, 0.1–0.2 ppm). We assume, by analogy to the slight differences observed in the crystal structure of a series of lanthanide-(III)-substituted thermolysins (Matthews & Weaver, 1974), that these $^1H$ NMR resonance shifts arise from small conformational changes in the protein when the lanthanides replace the native CD and EF site calcium ions.

In the case of the $Lu^{3+}$ titration (Figure 4), several of the methyl doublets (specifically, those centered at –0.362, 0.388, and 0.517 ppm) are gradually reduced in intensity by the progressive addition of lanthanide ion until, at $[Lu^{3+}]_0/[\text{parvalbumin}]_0$ ratios greater than about 2, they disappear.

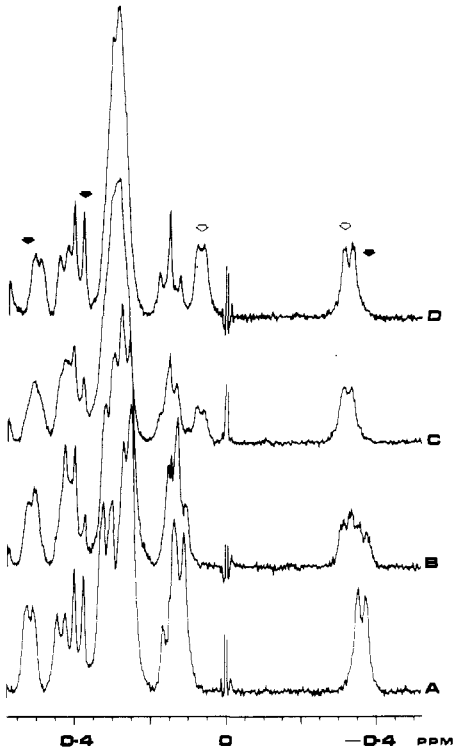


FIGURE 4: Upfield methyl region of selected $Lu^{3+}$ titration spectra of parvalbumin in 15 mM Pipes, 150 mM KCl, and 5 mM DTT, pH 6.8 and 55 °C, and referenced to DSS at the following ratios of $[Lu^{3+}]_0/[\text{parvalbumin}]_0$: (A) 0.00, (B) 0.85, (C) 1.70, and (D) 2.56 (only partial data shown). Peak heights of the resonances indicated by the arrows were normalized and plotted as a function of $[Lu^{3+}]_0/[\text{parvalbumin}]_0$ to determine the dissociation constants (relative to $Ca^{2+}$) for $Lu^{3+}$ from the CD and EF sites as described in the text (see Figure 6 and Table II).

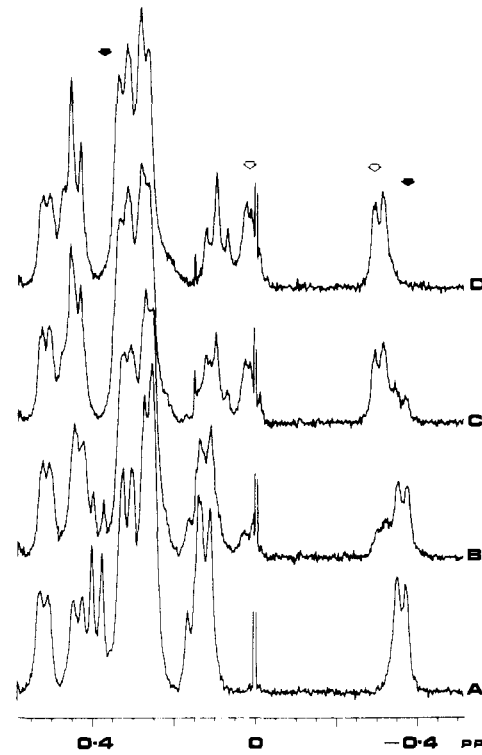


FIGURE 5: Upfield methyl region of selected $La^{3+}$ titration spectra of parvalbumin in 15 mM Pipes, 150 mM KCl, and 5 mM DTT and referenced to DSS at the following ratios of $[La^{3+}]_0/[\text{parvalbumin}]_0$: (A) 0.00, (B) 0.87, (C) 1.74, and (D) 2.60 (only partial data shown). Peak heights of the resonances indicated by arrows were normalized and plotted as a function of $[La^{3+}]_0/[\text{parvalbumin}]_0$ to determine the dissociation constants as described in the text (see Figure 7 and Table II).

Table II: Dissociation Constants for Lanthanides from Parvalbumin

| | $K^{CD}$ | $K^{EF}$ | $K_{D,Ln}^{CD}$ (M)[a] | $K_{D,Ln}^{EF}$ (M)[a] | comments |
|---|---|---|---|---|---|
| $La^{3+}$ | 0.005 | 0.012 | $2.0 \times 10^{-11}$ | $4.8 \times 10^{-11}$ | this work; 55 °C, pH 6.8 |
| $Yb^{3+}$ | 0.13 | 0.01 | $5.2 \times 10^{-10}$ | $4.0 \times 10^{-11}$ | Lee & Sykes (1981); 28 °C, pH 6.6 |
| $Lu^{3+}$ | 0.09 | 0.012 | $3.6 \times 10^{-10}$ | $4.8 \times 10^{-11}$ | this work; 55 °C, pH 6.8 |

[a] Absolute dissociation constants were calculated by using the dissociation constant ratios and a dissociation constant for calcium of $4.0 \times 10^{-9}$ M (Potter et al., 1977).

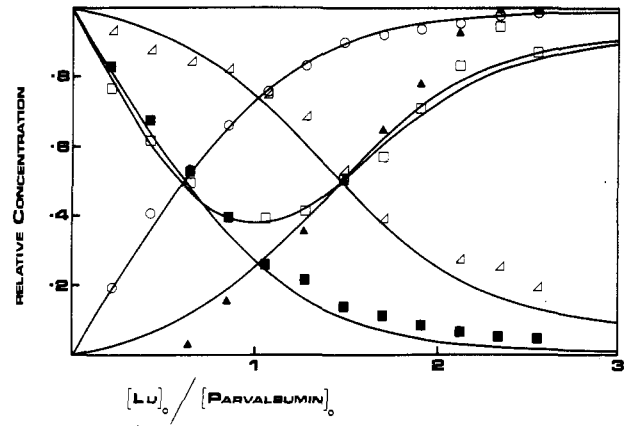


FIGURE 6: $Lu^{3+}$ titration of parvalbumin. Normalized peak heights of the five methyl resonances indicated in Figure 4 are plotted vs. the ratio $[Lu^{3+}]_0/[\text{parvalbumin}]_0$: −0.362 ppm (■); −0.325 ppm (○); 0.067 ppm (▲); 0.388 ppm (□); 0.517 ppm (△). Overlaying the data points are the theoretical curves showing the distribution of the parvalbumin species calculated from the dissociation constants obtained by a least-squares fit of the data (see Table II): species CC + LC (■); species CL + LL (○); species LL + LC (▲); species CC + LL (□); species CC + CL (△).

In addition, a number of resonances (specifically, those centered at −0.325 and 0.067 ppm, which are absent in the calcium spectrum) progressively increase in intensity to a maximum at a $[Lu^{3+}]_0/[\text{parvalbumin}]_0$ ratio of about 2. These changes in resonance intensities do not, however, appear to be synchronous: the rise of the resonance at 0.067 ppm clearly begins only after the rise in the resonance at −0.325 ppm and the correlated fall of the doublet at −0.362 ppm are nearly complete; in addition, the intensity of the 0.517 ppm doublet diminishes at a rate somewhat slower than the observed disappearance of the −0.362 ppm doublet. Especially striking is the behavior of the narrow doublet centered at 0.388 ppm, which, after first decreasing in intensity at a rate comparable to the disappearance of the −0.362 ppm doublet, begins to increase in intensity at a rate comparable to the appearance of the doublet at 0.067 ppm. These observations provide evidence for the coexistence of several different parvalbumin species and strongly suggest that the slow exchange of metal ions at the CD and EF sites is sequential. The relative dissociation constants, $K^{CD}$ and $K^{EF}$, for the binding of $Lu^{3+}$ to the two calcium sites of parvalbumin were calculated as described above (see Figure 6 and Table II).

The changes induced in the $^1H$ NMR spectrum of parvalbumin by $La^{3+}$ titration are in several respects quite similar to those changes observed for the $Lu^{3+}$ titration: the disappearance of the most upfield-shifted doublet resonance (at

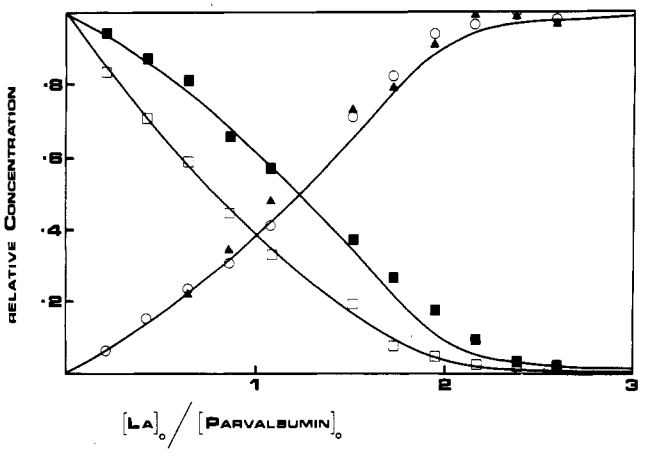


FIGURE 7: $La^{3+}$ titration of parvalbumin. Normalized peak heights of the four methyl resonances indicated in Figure 5 vs. the ratio $[La^{3+}]_0/[\text{parvalbumin}]_0$: −0.362 ppm (■); −0.302 ppm (○); 0.017 ppm (▲); 0.388 ppm (□). Overlaying the data points are the theoretical curves showing the distribution of parvalbumin species calculated from the dissociation constants obtained by a least-squares fit of the data (see Table II): species CC + LC (■); species LL + CL (○); species LL + CL (▲); species CC + CL (□);

−0.362 ppm) is again correlated to the rise of a doublet shifted just slightly downfield from it; the multiplet structure at about 0.13 ppm is again resolved into its doublet and triplet components; and the decrease in the intensity of the narrow doublet at 0.388 ppm observed for the initial phase of the $Lu^{3+}$ titration is again recorded for the $La^{3+}$ titration. More importantly, though, are the differences revealed by titration with $La^{3+}$. Analogous to the doublet resonances that arise sequentially during the $Lu^{3+}$ titration—one developing first at −0.325 ppm and a second coming later at 0.067 ppm—two doublet resonances appear simultaneously during the course of the $La^{3+}$ titration (at −0.302 and 0.017 ppm, respectively). Also the narrow doublet at 0.388 ppm does not regain, in the later phase of $La^{3+}$ titration, the intensity that it lost during the initial phase. Apparently, the binding of a second $La^{3+}$ ion does not shift this resonance back upfield sufficiently to make it appear as if it were going through two successive changes. The relative dissociation constants, $K^{CD}$ and $K^{EF}$, for the binding of $La^{3+}$ to the two calcium ion sites of parvalbumin were calculated as described above (see Figure 7 and Table II).

## Discussion

For a number of parvalbumins, $Ca^{2+}$ apparently binds to the CD and EF sites with indistinguishable affinities (Potter et al., 1977, 1978; Blum et al., 1977; Haiech et al., 1979). However, the kinetics of lanthanide ion release from $Ln^{3+}{}_2$-loaded carp parvalbumin, as determined here by stopped-flow techniques, reveal striking differences in the dissociation rate constants of these rare-earth ions from the CD and EF sites. Plotted as a function of the ionic charge density of the lanthanide ion (see Figure 1), the difference in the release rates from the two high-affinity sites, while quite pronounced for the heaviest lanthanides (i.e., $Yb^{3+}$ and $Lu^{3+}$), decreases in steady progression across the series, becoming irresolvable for $La^{3+}$ and the lightest lanthanides. Considering only this trend in the release rates of $Ln^{3+}$ ions from parvalbumin, one might tentatively suggest that the dissociation constants, $K_D$'s, for the lanthanides from the fast-release site would be essentially invariant across the series whereas the $K_D$'s for the slow-release site would dramatically decrease as one crossed from $La^{3+}$ to $Lu^{3+}$. However, an examination of the $K_D$'s calculated from the $^1H$ NMR monitored spectral changes of parvalbumin titrated with $La^{3+}$ and, in a separate experiment, $Lu^{3+}$ leads to a very different interpretation of the kinetic data.

For each of the two $^1H$ NMR titrations, two dissociation constant ratios ($K^{CD}$ and $K^{EF}$) were determined, one representing substitution of $Ca^{2+}$ by $La^{3+}$ or $Lu^{3+}$ at the CD site and the other representing substitution of $Ca^{2+}$ by $La^{3+}$ or $Lu^{3+}$ at the EF site. It was not, however, a priori apparent which constant from the $La^{3+}$ titration should be paired with which constant from the $Lu^{3+}$ titration to represent the binding of the two different lanthanides to the same protein site. Those residues sensitive only to $Ca^{2+}$ substitution at one site or the other provide a means of resolving the difficulty of properly pairing the calculated dissociation constants. A resonance arbitrarily attributed to a residue near one or the other $Ca^{2+}$ binding site by virtue of its intensity changes during titration with $La^{3+}$ (see Figures 5 and 7) must necessarily be attributed to that same residue—and, therefore, the same combination of parvalbumin–metal species—when the $Lu^{3+}$ titration results are evaluated (see Figures 4 and 6). For example, if the doublet resonance at −0.37 ppm in the $Ca^{2+}{}_2$ form of parvalbumin is arbitrarily included in the class of residues sensitive to only EF site exchange (its resonance intensity corresponding to the sum of CC and CL species; see Figure 3), then it must similarly be designated for both $La^{3+}$ and $Lu^{3+}$ titrations. When these constraints are imposed on the fitting routines previously described (see Results), one is lead to the conclusion that the dissociation constant ratio for one site remains unchanged (0.012 for both $La^{3+}$ and $Lu^{3+}$ relative to $Ca^{2+}$) whereas the dissociation constant ratio for the other site is much less for $La^{3+}$ than it is for $Lu^{3+}$ (0.005 compared to 0.090, both relative to $Ca^{2+}$). The relative binding affinities of these two sites undergo a reversal—i.e., if $La^{3+}$ is employed, it will bind more tightly to one site, whereas if $Lu^{3+}$ is used, it will bind more tightly to the other site.

In contradiction to the prediction based on the trend in $k_{off}$ that one of parvalbumin's high-affinity sites should show a marked preference for $Lu^{3+}$ over $La^{3+}$, the $K_D$'s indicate that the converse is true: although one site is insensitive to the nature of the bound lanthanide, the other site displays a 20–25-fold greater affinity for $La^{3+}$ compared to $Lu^{3+}$. Recourse to an examination of the rates of solvent exchange for the $Ln^{3+}$ ions provides a rationale for this apparent contradiction. Since all of the experimental work presented here was carried out in either $H_2O$ or $D_2O$, we will assume that the uncomplexed $Ln^{3+}$ ions were present as their aquocations with an inner hydration sphere of eight to nine water molecules (Ashcroft & Mortimer, 1970). Furthermore, it is usually agreed that the rate of lanthanide complex formation is primarily determined by the substitution rate of the first solvent molecule and is fairly insensitive to the nature of the ligand itself (Diebler et al., 1969; Hewkin & Prince, 1970). We will assume that trends in the on-rate constants, $k_{on}$, for lanthanide–parvalbumin complex formation can be closely approximately by the known trends in the $Ln^{3+}$–murexide complex formation rates (Geier, 1965). As can be seen in a plot of Geier's (1965) data (displayed as an inset in Figure 1), the trend from $La^{3+}$ to $Lu^{3+}$ is, for most of the series, a linear decrease in the rate of complex formation, which closely parallels the observed decrease in $k_{off}$ from the slow-release site of parvalbumin. If the dissociation constants for the slow site, in going from $La^{3+}$ to $Lu^{3+}$, are accompanied by similar decreases in the rates of complex formation (as seen for the formation of $Ln^{3+}$–murexide complexes), then the thermodynamically determined $K_D$ will remain constant. On the other hand, if $k_{off}$ remains nearly constant over the lanthanide series, as in the case of the fast-release site, then $K_D$ will decrease in going from $Lu^{3+}$

to $La^{3+}$. This interpretation, then, accounts both for the kinetics of the two-site release of lanthanide ions from $Ln^{3+}_2$–parvalbumin as well as for the apparent thermodynamic stabilities.

It is necessary to evaluate the temperature dependence of the kinetic and thermodynamic results since the $^1H$ NMR studies were conducted at 55 °C whereas the optical stopped-flow data were collected at 23 °C. It should first be noted that Lee & Sykes (1981), working at 30 °C and employing virtually identical $^1H$ NMR techniques, have previously calculated the $K_D$'s (relative to $Ca^{2+}$) for $Yb^{3+}$ at the CD and EF sites of carp parvalbumin to be 0.13 and 0.01, respectively. These $K_D$ values, which are quite similar to those obtained in this study for the binding of $Lu^{3+}$ to parvalbumin (whose analogous $K_D$ values are 0.090 and 0.012, respectively), suggest that, within this temperature range (approximately 20–55 °C), the dissociation constants of $Ln^{3+}$ ions from the CD and EF binding sites of parvalbumin do not change significantly. In addition, Figure 2 illustrates, in the form of an Arrhenius plot, the results of a study of the temperature dependence of the slow-release $k_{off}$ for the $Yb^{3+}$- and $La^{3+}$-substituted parvalbumins. The very small changes in log $k_{off}$ over the 20–55 °C temperature range noted for these end members of the lanthanide series translate into an activation energy of 2.6 kcal/mol for the release of $Yb^{3+}$ and 1.6 kcal/mol for the release of $La^{3+}$ from the slow site.

The observation that one of the two high-affinity metal binding sites of parvalbumin displays a range of affinities depending on which metal ion is bound whereas the other site is much less sensitive suggests that the apparently disparate results obtained by researchers in this field may be incorporated into a fairly simple picture of $Ln^{3+}$–parvalbumin complex formation. Because of their usefulness as luminescence probes, the lanthanide ions $Eu^{3+}$ and $Tb^{3+}$ have been employed to study the metal binding sites of a number of parvalbumins. For example, the $Eu^{3+}$ titration of the p$I$ 4.37 carp isozyme monitored by its excitation spectrum reveals an approximately equal filling of the two high-affinity sites (Rhee et al., 1981). Unfortunately, no $K_D$'s were reported for these $Eu^{3+}$–parvalbumin complexes. In addition, $Gd^{3+}$ has also been used to probe the CD and EF sites of parvalbumin. Cavé et al. (1979), using the method of proton relaxation enhancement, were unable to distinguish between the binding of $Gd^{3+}$ at the CD and EF sites, reporting what they felt represented an average $K_D$ for the two sites ($K_D = 0.5 \times 10^{-11}$ M). These results are in complete agreement with the predicted crossover in binding affinities at some point in the series, presumably near the middle members. This result has also been seen in the displacement of $^{113}Cd$ from $Cd_2$-substituted parvalbumin by various lanthanides (Vogel et al., 1983).

Smolka et al. (1971) and Darnall & Birnbaum (1973) have shown not only that lanthanide(III) ions functionally replace the four calcium ions of native *Bacillus subtillus* $\alpha$-amylase but also that they do so with varying degrees of success. Whereas $Lu^{3+}$ completely reactivated apo-$\alpha$-amylase, the potential of the other lanthanides to do so decreased across the series ($Lu^{3+} \rightarrow La^{3+}$) in a linear fashion when plotted against their respective ionic radii. That $Ln^{3+}$ ions do indeed serve as good substitutes for $Ca^{2+}$, as might otherwise be expected from their similar ionic sizes (0.85–1.15-Å range of ionic radii for the lanthanides compared to a 0.99-Å radius for $Ca^{2+}$) and similar strong preferences for complexing with oxygen ligands, is further supported by the closeness with which the measured $k_{off}$ for $Ca^{2+}$ release from parvalbumin fits to the line describing the release of $Ln^{3+}$ ions from the slow site. Since Donato & Martin (1974) have shown that limited dialysis of $Ca^{2+}$-saturated parvalbumin against EGTA–buffer appears to remove only one of the two bound $Ca^{2+}$ ions, one might predict that the $Ca^{2+}$-saturated parvalbumin should display not one but rather two discrete $K_D$'s, one for each of the CD and EF sites.

## Acknowledgments

We acknowledge the help of several people: Dr. R. Stewart for help with isoelectric focusing, Dr. W. McCubbin and K. Oikawa for advice on preparations and use of their spectrometer, M. Nattriss for amino acid analysis, and D. Dombrowski and J. Shelling for advice with preparations and metal ion solutions. We are especially indebted to Drs. T. Drakenberg and S. Forsén (Lund) for many helpful discussions and communicating their results prior to publication.

**Registry No.** La, 7439-91-0; Pr, 7440-10-0; Nd, 7440-00-8; Sm, 7440-19-9; Eu, 7440-53-1; Gd, 7440-54-2; Tb, 7440-27-9; Dy, 7429-91-6; Ho, 7440-60-0; Er, 7440-52-0; Tm, 7440-30-4; Yb, 7440-64-4; Lu, 7439-94-3; Ca, 7440-70-2.

## References

Ashcroft, S. J., & Mortimer, C. T. (1970) *Thermochemistry of Transition Metal Complexes*, Chapter 12, Academic Press, London.

Birnbaum, E. R., & Sykes, B. D. (1978) *Biochemistry 17*, 4965.

Blum, H. E., Lehky, P., Kohler, L., Stein, E. A., & Fischer, E. H. (1977) *J. Biol. Chem. 252*, 2834.

Cavé, A., Daures, M.-F., Parello, J., Saint-Yves, A., & Sempere, R. (1979) *Biochimie 61*, 755.

Corson, D. C., Lee, L., McQuaid, G. A., & Sykes, B. D. (1983) *Can. J. Biochem. Cell. Biol. 61*, 860.

Darnall, D. W., & Birnbaum, E. R. (1970) *J. Biol. Chem. 245*, 6484.

Darnall, D. W., & Birnbaum, E. R. (1973) *Biochemistry 12*, 3489.

Diebler, H., Eigen, M., Ilgenfritz, G., Maass, G., & Winkler, R. (1969) *Pure Appl. Chem. 20*, 93.

Donato, H., Jr., & Martin, R. B. (1974) *Biochemistry 13*, 4575.

Geier, V. G. (1965) *Ber. Bunsenges. Phys. Chem. 69*, 617.

Haiech, J., Derancourt, J., Pechère, J.-F., & Demaille, J. G. (1979) *Biochimie 61*, 583.

Heizman, C. W., & Strehler, E. E. (1979) *J. Biol. Chem. 254*, 4296.

Hewkin, D. J., & Prince, R. H. (1970) *Coord. Chem. Rev. 5*, 45.

Hunt, J. B., & Ginsburg, A. (1981) *Biochemistry 20*, 2226.

Kretsinger, R. H., & Nockolds, C. E. (1973) *J. Biol. Chem. 248*, 3313.

Kretsinger, R. H., & Nelson, D. J. (1976) *Coord. Chem. Rev. 18*, 29.

Lee, L., & Sykes, B. D. (1981) *Biochemistry 20*, 1156.

Martin, R. B., & Richardson, F. S. (1979) *Q. Rev. Biophys. 12*, 181.

Matthews, B. W., & Weaver, L. H. (1974) *Biochemistry 13*, 1719.

Miller, T. L., Cook, R. M., Nelson, D. J., & Theohardies, A. D. (1980) *J. Mol. Biol. 141*, 223.

Moews, P. C., & Kretsinger, R. H. (1975) *J. Mol. Biol. 91*, 229.

Nelson, D. J., Miller, T., L., & Martin, R. B. (1977) *Bioinorg. Chem. 7*, 325.

Pechère, J. F., Demaille, J., & Capony, J. P. (1971) *Biochim. Biophys. Acta 236*, 391.

Potter, J. D., Johnson, J. D., Dedman, J. R., Schrieber, W. E., Mandel, F., Jackson, R. L., & Means, A. R. (1977) in *Calcium Binding Proteins and Calcium Function* (Wasserman, R. J., Corradino, R. A., Carafoli, E., Kretsinger, R. H., MacLennan, D. H., & Siegel, F. L., Eds.) pp 239–249, Elsevier, New York.
Potter, J. D., Johnson, J. D., & Mandel, F. (1978) *Fed. Proc., Fed. Am. Soc. Exp. Biol. 37*, 1608.
Rhee, M.-J., Sudnick, D. R., Arkle, V. K., & Horrocks, W. deW., Jr. (1981) *Biochemistry 20*, 3328.
Shannon, R. D. (1976) *Acta Crystallogr., Sect. A: Cryst. Phys., Diffr., Theor. Gen. Crystallogr. A32*, 751.
Smolka, G. E., Birnbaum, E. R., & Darnall, D. W. (1971) *Biochemistry 10*, 4556.
Sowadski, J., Cornick, G., & Kretsinger, R. H. (1978) *J. Mol. Biol. 124*, 123.
Tonosaki, K., & Otamo, M. (1962) *Bull. Chem. Soc. Jpn. 35*, 1683.
Vogel, H. J., Drakenberg, T., & Forsén, S. (1983) in *NMR of Quadrapolar and Less Receptive Nuclei with Chemical and Biochemical Applications* (Laszlo, P., Ed.) Academic Press, New York.

# Essential Histidyl Residues of Ferredoxin–NADP$^+$ Oxidoreductase Revealed by Diethyl Pyrocarbonate Inactivation†

Néstor Carrillo and Rubén H. Vallejos*

ABSTRACT: Diethyl pyrocarbonate inhibited diaphorase activity of ferredoxin–NADP$^+$ oxidoreductase with a second-order rate constant of 2 $mM^{-1}\cdot min^{-1}$ at pH 7.0 and 20 °C, showing a concomitant increase in absorbance at 242 nm due to formation of carbethoxyhistidyl derivatives. Activity could be restored by hydroxylamine, and the pH curve of inactivation indicated the involvement of a residue having a p$K_a$ of 6.8. Derivatization of tyrosyl residues was also evident, although with no effect on the diaphorase activity. Both NADP$^+$ and NADPH protected the enzyme against inactivation, suggesting that the modification occurred at or near the nucleotide binding domain. The reductase lost all of its diaphorase activity after about two histidine residues had been blocked by the reagent. In differential-labeling experiments with NADP$^+$ as protective agent, it was shown that diaphorase inactivation resulted from blocking of only one histidyl residue per mole of enzyme. Modified reductase did not bind pyridine nucleotides. Modification of the flavoprotein in the presence of NADP$^+$, i.e., with full preservation of diaphorase activity, resulted in a significant impairment of cytochrome *c* reductase activity, with a second-order rate constant for inactivation of about 0.5 $mM^{-1}\cdot min^{-1}$. Reversal by hydroxylamine and spectroscopic data indicated that this second residue was also a histidine. Ferredoxin afforded only slight protection against this inhibition. Conversely, carbethoxylation of the enzyme did not affect complex formation with the ferrosulfoprotein. Redox titration of the modified reductase with NADPH and with reduced ferredoxin suggested that the second histidine might be located in the electron pathway between FAD and ferredoxin. On the basis of these results, two different types of essential histidyl residues can be distinguished in ferredoxin–NADP$^+$ oxidoreductase: One of them appears to be related with the nucleotide binding site, presumably behaving as a positive counterpart for the anionic molecule of NADP$^+$. The second, less reactive, histidine residue may be involved in the electron transport between ferredoxin and the flavin moiety.

Ferredoxin–NADP$^+$ oxidoreductase (EC 1.18.1.2) is a FAD[1]-containing enzyme that operates as the terminal acceptor of the photosynthetic electron transport chain in algae and higher plants. The membrane-bound flavoprotein catalyzes the reversible reduction of NADP$^+$ by ferredoxin (Shin & Arnon, 1965). Quite recently, Shahak et al. (1981) have suggested that it might also participate in the cyclic electron flow around photosystem I. The enzyme was initially described as a NADPH-specific diaphorase by Avron & Jagendorf (1956) and first isolated in a crystalline form by Shin et al. (1963).

The flavoprotein was shown to be located on the outer surface of the thylakoid membrane is a wide variety of photosynthetic organisms (Berzborn, 1968; Bohme, 1978; Rowell et al., 1981) with its catalytic site facing the chloroplast stroma. The attachment to, or solubilization from, the membrane results from a compromise between van der Waals attractive forces and Coulombic repulsion (Carrillo & Vallejos, 1982). The membrane-bound form of the enzyme undergoes a light-driven conformational change (Carrillo et al., 1980; Wagner et al., 1982) that may play a role in the activation of the photosynthetic electron transport during dark–light transitions (Satoh & Katoh, 1980; Carrillo et al., 1981b; Satoh, 1981; Carrillo & Vallejos, 1983b).

In addition to its physiological role in electron transport, the reductase, either in its soluble or membrane-bound form, is able to mediate several other reactions, including the oxidation of NADPH by artificial electron acceptors (diaphorase

† From the Centro de Estudios Fotosintéticos y Bioquímicos, Suipacha 531, 2000 Rosario, Argentina. *Received March 14, 1983.* This work was supported by grants from the Consejo Nacional de Investigaciones Científicas y Técnicas, Fund. M. Lillo, U.N. de Rosario, Argentina. R.H.V. is a Career Investigator member, and N.C. is a Fellow of the same institution.

[1] Abbreviations: Tris, tris(hydroxymethyl)aminomethane; DEAE, diethylaminoethyl; NBD-Cl, 7-chloro-4-nitro-2,1,3-benzoxadiazole; Fd, ferredoxin; DCPIP, 2,6-dichlorophenolindophenol; FeCy, potassium ferricyanide; FAD, flavin adenine dinucleotide; NADP$^+$, oxidized nicotinamide adenine dinucleotide phosphate; NADPH, reduced nicotinamide adenine dinucleotide phosphate.

0006-2960/83/0422-5889$01.50/0 